

Hou et al., 2017, Recycling of metal-fertilized lower continental crust: Origin of non-arc Au-rich porphyry deposits at cratonic edges: Geology, doi:10.1130/G38619.1.

Petrography of xenoliths

These xenoliths are black, rounded, and variably-sized (3–10 cm in diameter), with sharp boundaries that lack quench margins (Fig. 2a, b).

Garnet-amphibolite

The garnet-amphibolites have variable modal abundance, consisting of amphibole (50–65 vol. %), garnet (10–15 vol. %), diopside (5–15 vol. %), titanite (5–10 vol. %), and minor biotite (~5 vol. %), albite (2–5 vol. %), and magnetite/sulfides (~1 vol. %) (Figs. 2d, DR1a). Garnets are rich in Al_2O_3 and FeO , and have a relatively high abundance of almandine ($\text{Pyr}_{23-26}\text{Gro}_{18-24}\text{Alm}_{41-51}$, Table DR8), suggesting an origin in high-pressure garnet-granulite facies metamorphism. Amphibole formed in two generations: early brown Fe-rich pargasite (Am (I)) coexisting with garnet, and later green pargasite (Am (II)) forming during retrograde metamorphism (Fig. 2d, Table DR4). Coarse-grained diopside is Al-rich and has a relatively high Tschermaks' [$\text{CaAl}_2\text{SiO}_6$] component ($\text{Wo}_{43-46}\text{En}_{32-41}\text{Fs}_{12-19}$, Table DR3), whereas biotite is rich in MgO with a relatively high magnobiotite component (Table DR9). Biotite intergrows with the late green pargasite (Am (II)), which are the latest alteration products including garnet and diopside (Fig. DR1a). Chalcopyrite and pyrrhotite are the main sulfide species in garnet amphibolites (Fig. DR1c).

Amphibolite

The amphibolites also show variable modal abundance, composed of amphibole (40–60 vol. %), feldspar (30–38 vol. %), and biotite (3–10 vol. %) with minor sulfide phases (0.5–1.0 vol. %). Amphiboles have relatively high edenite component (Table DR4), suggesting an origin in high-amphibolite facies metamorphism. The Beiya amphibolites have high modal

biotite (10 vol. %) and contain more orthoclase (35–38 vol. %) than albite in Liuhe amphibolites (Fig. DR1b, Table DR10), implying secondary replacement by K₂O-rich fluids. Chalcopyrite and pyrite are the main sulfide species in amphibolites (Fig. DR1d).

Alteration

The Beiya amphibolite xenoliths contrast with those from the Liuhe stock, and show strong enrichment in Cu (383–445 ppm) and Au (7–12 ppb; Table DR6). The irregular shape of interstitial chalcopyrites, gold-rich pyrites, intense overprinting of secondary biotite, high LOI (e.g., LOI > 5.9 wt. %), and abnormal K₂O and other LILE contents (Table DR6) in these xenoliths indicate that the Cu (Au) enrichment was likely caused by introduction of external Cu (Au)-rich fluids. Possibly related to the Eocene mineralization processes.

Figure captions:

Fig. DR1 The xenoliths and their mineral assemblages. (a) Two generations of amphibole and diopsidite are visible in garnet amphibolite sample. (b) Amphibolite xenolith (Sample BYB15-2-1), consisting of amphibole, orthoclase and biotite. (c) Backscattered electron (BSE) images of a globular sulfide trapped in garnet grain coexisting with Am (I) and plagioclase in a garnet-amphibolite xenolith (Sample LH151-1). (d) BSE images of pyrite and chalcopyrite with orthoclase and biotite in amphibolite xenolith. (e) symplektitic crystallite of magnetite and pargasite around garnet grains; (f) fine-grained green amphibole and magnetite are around or within coarse-grained diopsidite; (g) comb-like fine-grained magnetite-amphibole rims around garnet; (h) fine-grained magnetite on the rim of garnet. Abbreviations: Am = amphibole, Ap = apatite, Bi = biotite, Cp = chalcopyrite, Di = diopsidite, Gt = garnet, Hb = hornblende, Mt = magnetite, Or = orthoclase, Pl = plagioclase, Po = pyrrhotite, Py = pyrite, Qtz = quartz, and Rt = rutile.

Fig. DR2 Zircon ages of the xenoliths and their host rocks. (a) Comparison of zircon age population of the Beiya amphibolite xenoliths (red) with Neoproterozoic arc plutons (blue) in the western Yangtze Craton. Inset map shows a weighted mean $^{206}\text{Pb}/^{238}\text{U}$ age of 37.9 ± 0.8 Ma for magmatic zircons from the host monzogranite at Beiya. (b). Comparison of zircon age distribution between the Liuhe garnet-amphibolite xenoliths (red) and Neoproterozoic arc plutons (blue). Inset map shows a weighted mean $^{206}\text{Pb}/^{238}\text{U}$ age of 34.6 ± 0.4 Ma for magmatic zircons from the host syenites at Liuhe. (c). Concordia plots for all zircons from the Liuhe garnet-amphibolite xenoliths. Metamorphic zircons ($n = 5$) yield an old weighted mean $^{206}\text{Pb}/^{238}\text{U}$ age of 794 ± 11 Ma (left inset), whereas fine-grained rounded zircons (e.g., 36.9 ± 0.1 Ma; Th/U = 0.06) and rims around old zircon grains yield a young weighted mean $^{206}\text{Pb}/^{238}\text{U}$ age of 35.6 ± 0.4 Ma (right inset). Inset photos in (a-c) show cathodoluminescence images of representative zircons with spot locations marked. Zircon ages were determined by SHRIMP II (Table DR5). Uncertainties in ages are quoted at the 95% confidence level (2σ).

Fig. DR3 Chondrite-normalized trace element diagrams for Beiya xenolith Neoproterozoic magmatic zircons, Beiya xenolith Neoproterozoic metamorphic zircons, Liuhe xenolith Neoproterozoic magmatic zircons, and Liuhe xenolith Cenozoic magmatic zircons. Notice that the Beiya Neoproterozoic metamorphic zircons have flat HREE patterns, suggesting their crystallization with the presence of garnet. Data are listed in Table DR11.

Fig. DR4 Geochemical affinity of the xenoliths with the Neo-proterozoic arc rocks. SiO_2 vs. Zr/Ti plot (a), Sr/Y vs. Y plot (b), and trace element abundance patterns (c), illustrating that the xenoliths have similar trace element patterns and show geochemical affinity with Neo-proterozoic arc rocks. The pre-mineralized porphyries are best reproduced by melting of 10% Garnet amphibolite, whereas the mineralized porphyries are best reproduced by melting of

eclogitic to amphibole-eclogitic material. Trends A, B and C in (b) reflect compositional variations of distinct melts produced by melting of eclogite (am/cpx = 50/50), amphibole eclogite (gt/am/cpx = 40/10/50) and garnet amphibolite (gt/am = 10/90), respectively. Partitioning coefficient of Y and Sr in mineral(i.e. amphibole, clinopyroxene and garnet) are from Arth (1976).Partitioning coefficient (D) of Sr and Y are 0.036 and 4.95 for eclogite, 0.08 and 4.15 for amphibole eclogite, 0.41 and 1.81 for garnet amphibolite, respectively. Data source: the Beiya fertile porphyries from (He, 2014), 740-1000Ma arc plutons from (Zhao et al., 2007), and others from Table DR6. The simulation was finished based on the model of batch melting($C_L D_i(1-F)+F=C_0$). Am = amphibole, Cpx = clinopyroxene, Gt = garnet.

Fig. DR5 Zircon $Hf(t)$ vs. U-Pb age plot for the xenoliths and their host rocks. Dashed line represents the evolution trend of Neo-proterozoic mafic rocks (Zhao and Zhou, 2007) and the lower-crustal xenoliths at 0.9, 1.1 and 1.3Ga, assuming that the xenoliths and unexposed complementary mafic cumulates to these arc rocks have a Lu/Hf ratio similar to that of a global mafic lower crust ($^{176}\text{Lu}/^{177}\text{Hf}$ ratio ~ 0.022). The gray band shows that the Beiya Au-rich porphyries could be derived by remelting juvenile mafic lower crust dominated by cumulates (i.e., Liuhe xenoliths) of the Neo-proterozoic arc magmas. Data listed in Table DR11.

Fig. DR6 Plots of for the amphibolite xenoliths illustrating Cu-Au rich samples have high contents of LILEs and LOIs. All data are listed in Table DR10

Tables

Table DR1 EPMA compositions of oxides and sulfides in the Liuhe and Beiya xenoliths

Table DR2 LA-ICPMS compositions of oxides and sulfides in the Liuhe xenoliths

Table DR3 Chemical compositions and estimated P-T conditions of pyroxenes in the Liuhe xenoliths

Table DR4 Chemical compositions of amphiboles in the xenoliths at Liuhe and Beiya

Table DR5 U-Pb ages of zircons from the xenoliths and their host rocks at Beiya and Liuhe

Table DR6 Whole-rock chemical analyses of the xenoliths and host rocks of Beiya and Liuhe in the western Yangtze Craton

Table DR7 Zircon Lu–Hf isotope data of the Liuhe xenolith and syenite

Table DR8 Chemical compositions of garnets in the Liuhe xenoliths

Table DR9 Chemical compositions of micas in the Liuhe and Beiya xenoliths

Table DR10 Chemical compositions of feldspars in the Liuhe and Beiya xenoliths

Table DR11 Zircon trace element compositions of Liuhe and Beiya xenoliths

References

Amelin, Y., Lee, D.C., Halliday, A.N. and Pidgeon, R.T., 1999, Nature of the Earth's earliest crust from hafnium isotopes in single detrital zircons: *Nature*, v. 399, p. 252–255.

Arth, J.G., 1976, Behaviour of trace elements during magmatic process- a summary of theoretical model and their application: *Res. U.S.Geol.Surv*, v.4, p.41-47

Barth, T.W., 1952, *Theoretical petrology: a textbook on the origin and evolution of rocks*: New York, Wiley.

Black, L.P., Kamo, S.L., Allen, C.M., Aleinikoff, J.N., Davis, D.W., Korsch, R.J. and Foudoulis, C., 2003, A new zircon standard for Phanerozoic U–Pb geochronology: *Chem. Geol*, v. 200, p. 155–170.

Defant, M.J. and Drummond, M.S., 1990, Derivation of some modern arc magmas by melting of young subducted lithosphere: *Nature*, v. 347, p. 662-665.

- Griffin, W.L., Powell, W.J., Pearson, N.J. and O'Reilly, S.Y., 2008, GLITTER: data reduction software for laser ablation ICP-MS. In: Laser Ablation-ICP-MS in the Earth Sciences (P. Sylvester, ed.): Mineralogical Association of Canada Short Course Series Volume 40, Appendix 2, p. 204-207.
- He, W.Y., 2014, The Beiya giant dold-polymetallic deposit: Magmatism and metallogenic model. Unpub. PhD dissertation, China University of Geosciences, p. 1–159 (in Chinese with English abstract).
- Mercier, J.C., 1980, Single-pyroxene thermobarometry: Tectonophysics, v. 70, p. 1- 37.
- Ravna, E.K., 2000, The garnet-clinopyroxene Fe^{2+} -Mg geothermometer: an updated calibration: Jour. Metamorphic Geol., v. 18, p. 211- 219.
- Schmit M.W., 1992, Amphibole composition in tonalite as a function of pressure: An experiment alcalibration of the A-l in-hornblend barometer: Contrib Mineral Petrol, v. 110, p. 304-310.
- Sun, S.H. and Yu, J., 1989, Interpretation of chemical composition and subdivision of Mg-Fe micas, part b: the natural subdivision of Mg-Fe micas: Chinese Journal of Geology, v. 2, p. 176-188 (in Chinese with English abstract).
- Williams, I.S., 1992, Some observations on the use of zircon U-Pb geochronology in the study of granitic rocks: Trans. R. Soc. Edinburgh-Earth Sci., v. 83, p. 447-458.
- Zhao, X., Yu, X.H., Mo, X.X., Zhang, J. and Lu, B.X., 2004, Petrological and geochemical characteristics of Cenozoic lakalic-rich porphyries and xenoliths hosted in western Yunnan Province: Geoscience, v. 18, p. 217–228 (in Chinese with English abstract).

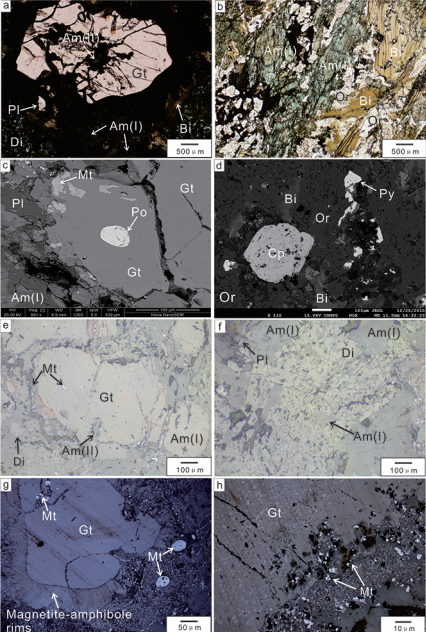
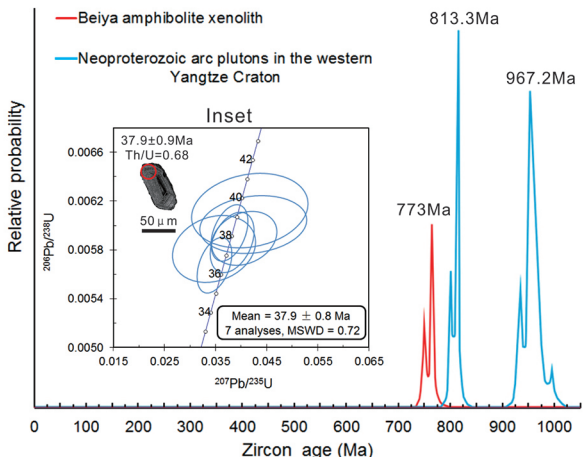
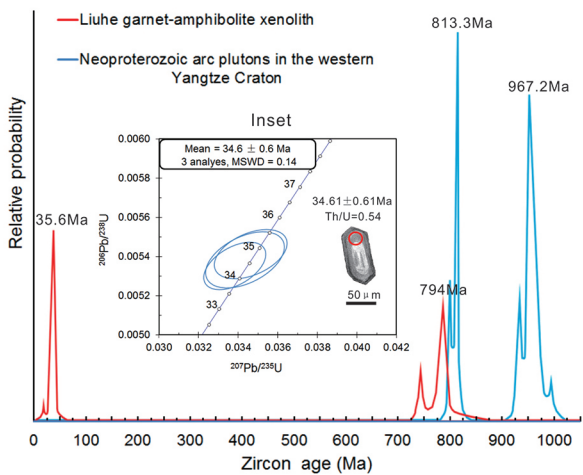


Fig. DR1

a



b



c

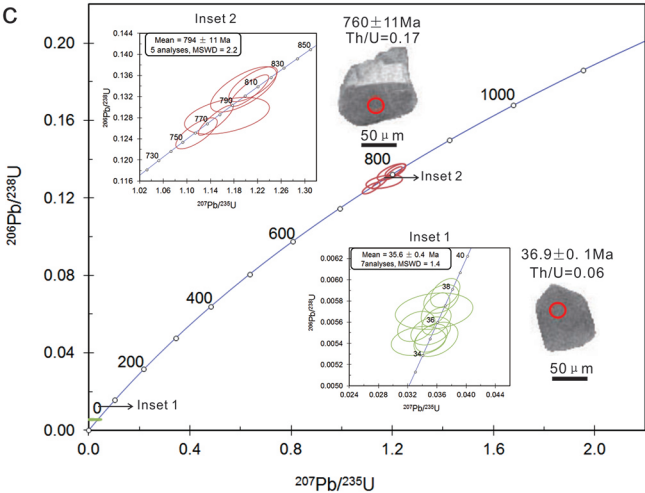


Fig. DR2

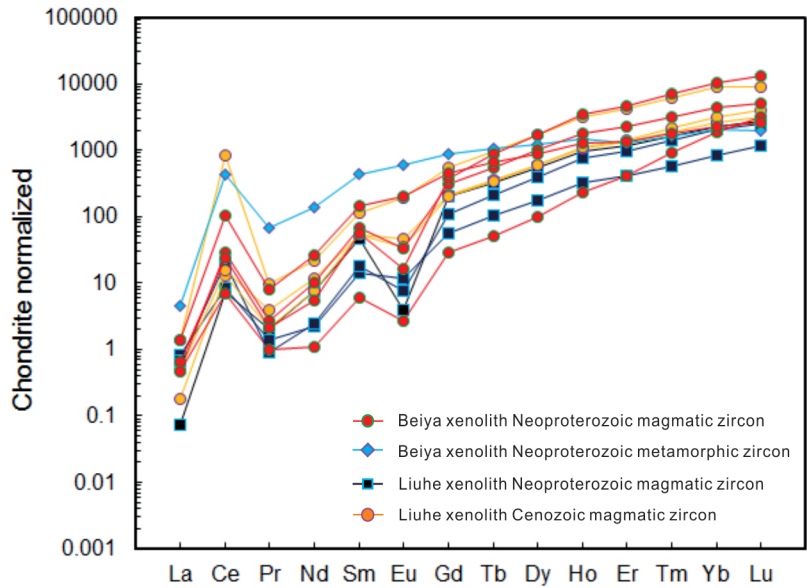


Fig.DR3

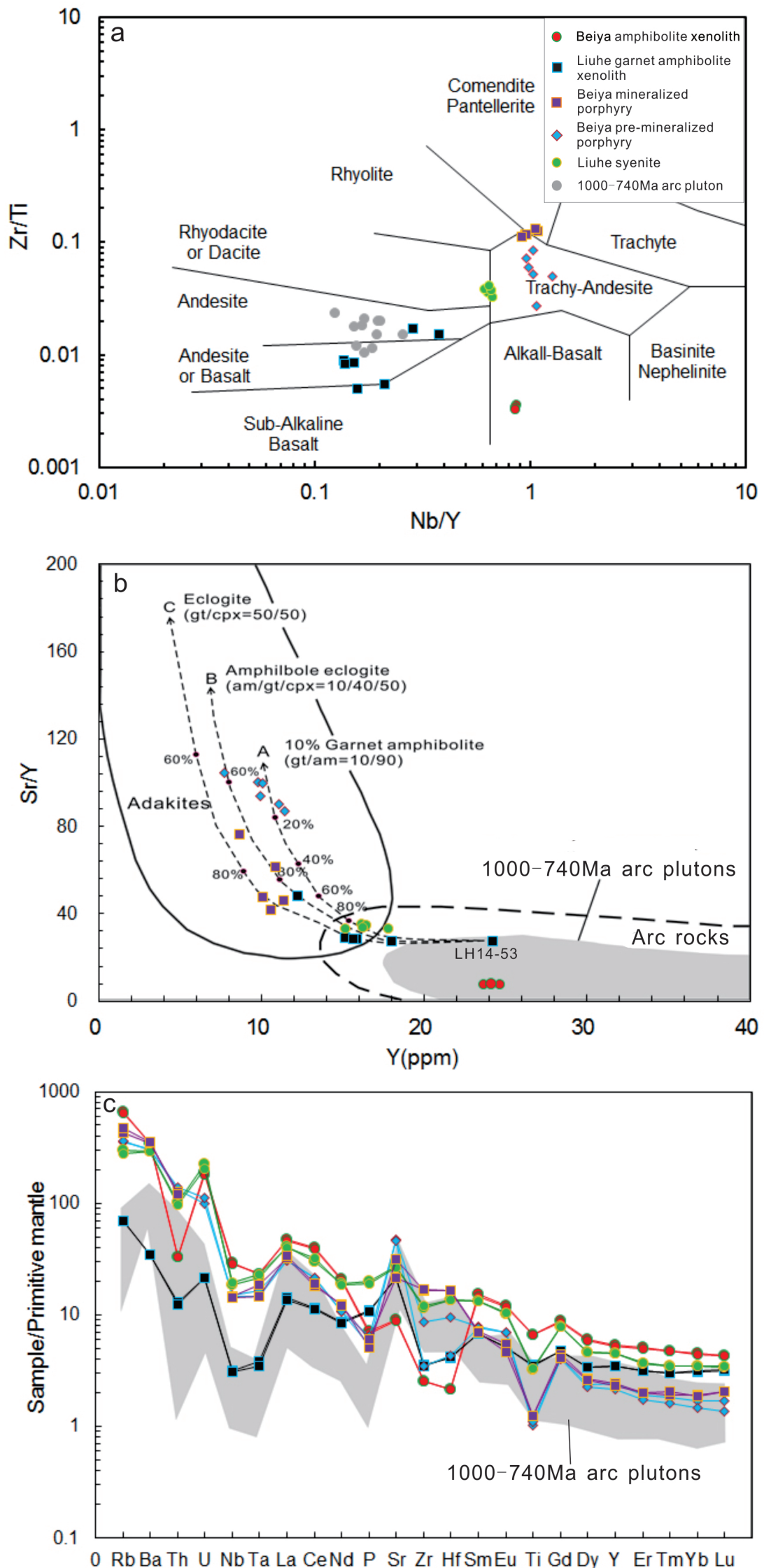


Fig. DR4

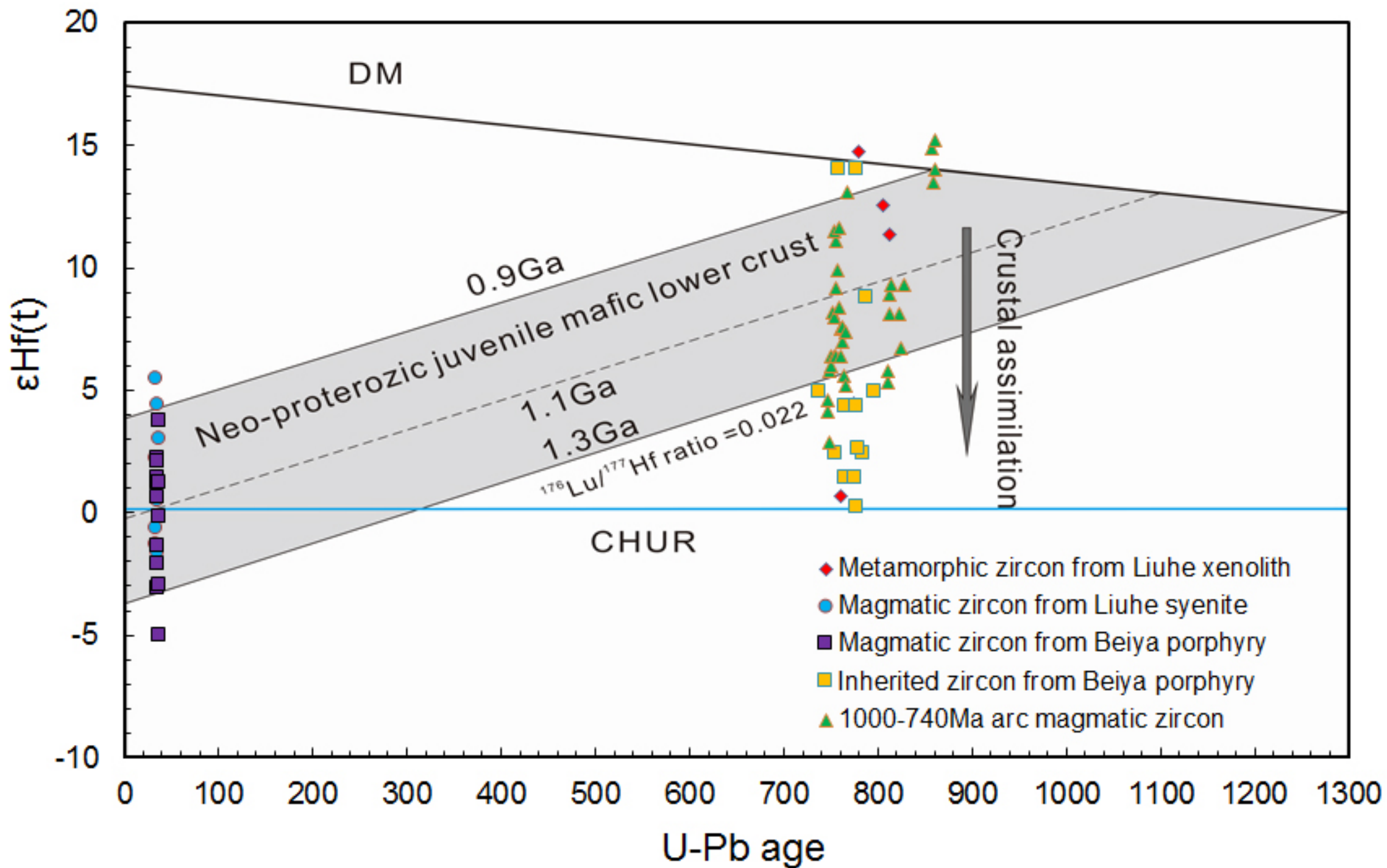


Fig.DR5

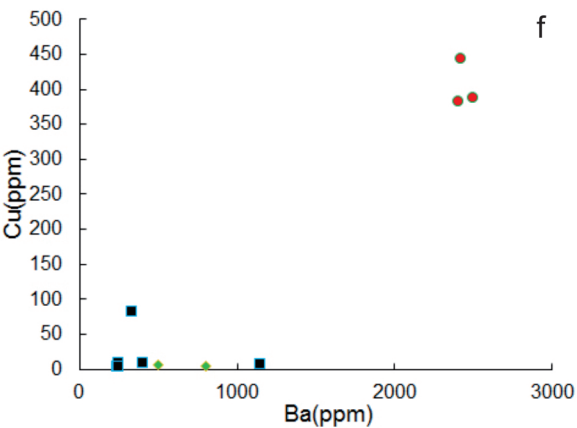
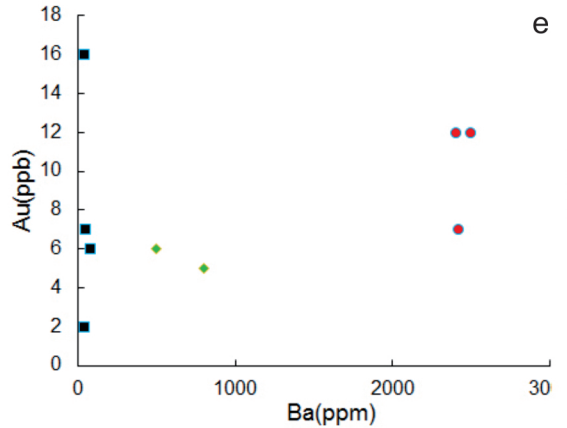
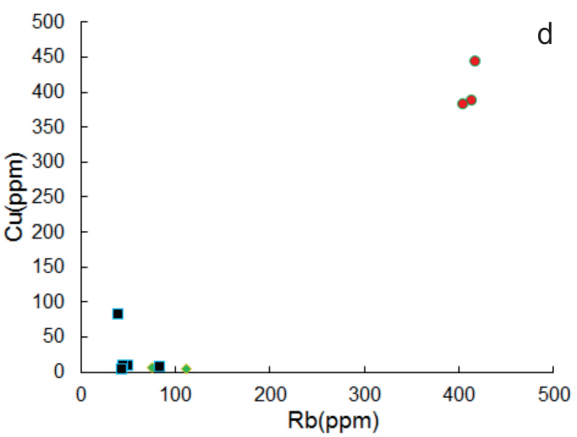
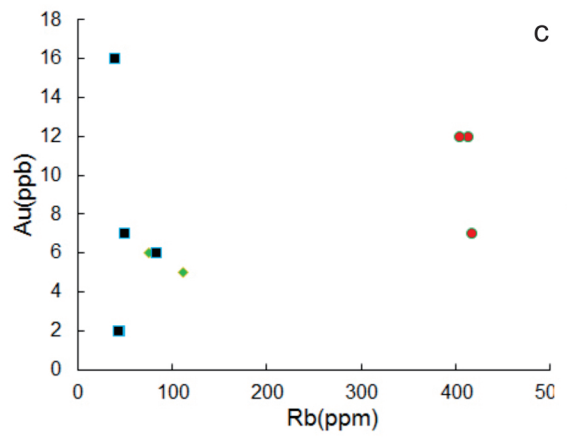
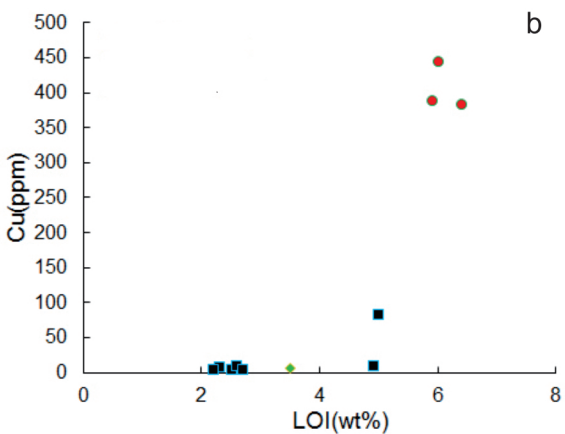
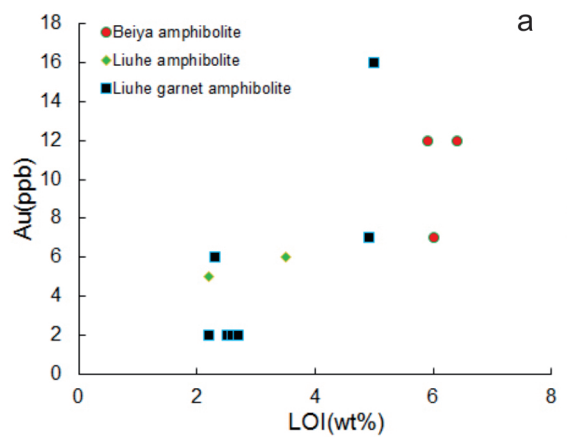


Fig.DR6

Table DR1 EPMA compositions of oxides and sulfides in the Liuhe and Beiya xenoliths

Chemical compositions of oxides												
Sample	Lithology	Mineral	SiO ₂	TiO ₂	Al ₂ O ₃	FeO	MnO	MgO	CaO	Na ₂ O	K ₂ O	P ₂ O ₅
LH14-57	Garnet amphibolite	Rutile	0.03	97.67	0.03	1.21	0.04	0.00	0.02	0.00	0.00	0.00
LH14-57	Garnet amphibolite	Ilmenite	0.03	46.77	0.03	46.84	1.95	1.28	0.03	0.00	0.01	0.00
LH14-57	Garnet amphibolite	Magnetite	4.40	0.00	0.17	89.13	0.04	0.06	0.03	0.07	0.00	0.01
LH14-24	Garnet amphibolite	Magnetite	0.17	2.01	2.51	87.33	2.03	0.31	0.04	0.13	0.01	0.00
LH14-24	Garnet amphibolite	Magnetite	0.15	0.69	2.68	88.66	2.18	0.50	0.00	0.06	0.01	0.03
LH5-1	Garnet amphibolite	Magnetite	0.15	0.69	2.68	88.66	2.18	0.50	0.00	0.06	0.01	0.03

Chemical compositions of sulfides												
Sample	Lithology	Mineral	As	Fe	Cu	S	Co	Ni	Zn	Ag	Au	Te
LH14-57	Garnet amphibolite	Pyrite	2.3730	46.4440	0.0180	51.8060	0.0610	0.0000	0.0270	0.0000	0.0190	0.0000
LH14-57	Garnet amphibolite	Pyrrhotite	0.4200	58.5450	0.2680	40.1420	0.0110	0.0000	0.0040	0.0000	bdl	0.0000
LH5-1	Garnet amphibolite	Pyrrhotite	0.6800	60.8700	0.2680	38.2630	0.0110	0.0000	0.0098	0.0000	bdl	0.0000
LH5-1	Garnet amphibolite	Chalcopyrite	0.0020	30.3820	34.0310	34.7330	0.0000	0.0000	0/0081	0.0000	bdl	0.0000
LH14-24	Garnet amphibolite	Pyrite	2.4220	46.8590	0.0310	51.1230	0.0880	0.0000	0.0310	0.0120	0.0580	0.0150
BYB15-2-1	Amphibolite	Chalcopyrite	0.0030	29.2530	35.0360	34.9220	0.9140	0.0120	0.0670	0.0000	bdl	0.0000
BYB15-2-1	Amphibolite	Pyrite	0.0060	44.8990	0.0310	53.4380	1.0470	0.0000	0.0000	0.0170	0.0000	

Note: The chemical composition of minerals were determined by electron microprobe analysis (EMPA) using a Jeol JXA-8230 at the Institute of Mineral Resources, Chinese Academy of Geological Sciences. The operating conditions were accelerating voltage of 15 kV for silicate and oxide, and 20kV for sulfide, beam current of 20 nA and beam size of 5 μm . Natural minerals and synthetic materials were used as standards, and all of the standards were tested for homogeneity before their utilization for quantitative analysis. Matrix corrections were carried out using the ZAF correction program supplied by the manufacturer. The detection limit for Au is 0.014 wt. % and for Cu is 0.016 wt. %, bdl = below of detection limit.

Table DR2 LA-ICPMS compositions of oxides and sulfides in the Liuhe xenoliths

Sample	Lithology	Mineral	ppm	Au	Cu	S	As	Ni	Zn	Ag	Co
LH14-46	Garnet amphibolite	Pyrite		0.07	2253	11110	518.0	20890	3260	0.55	43.00
LH14-46	Garnet amphibolite	Pyrite	bdl	924	76200	471.00	12560	122.9	2.43	16.00	
LH14-46	Garnet amphibolite	Pyrite	0.11	8600	4390	156.80	25890	1180	3.78	1.70	
LH5-1	Garnet amphibolite	magnetite	bdl	11.6	0.01	5.20	46.60	707.0	0.01	8.90	
LH5-1	Garnet amphibolite	magnetite	bdl	124	0.01	4.50	41.40	859.0	0.01	4.70	
LH5-1	Garnet amphibolite	Pyrrhotite	bdl	3270	360000.00	0.88	2626.00	16.51	0.42	74.00	

Note: LA-ICP-MS for in situ trace element analysis of pyrite, magnetite, and pyrrhotite was performed on thinsections in the GeoHistory Facility of the John de Laeter Centre, Curtin University, Perth in Australia. The analysis utilized a Resonetics RESOlution M-50A-LR incorporating a Compex 102 excimer laser, coupled to an Agilent 7700s quadrupole ICP-MS. Following a 20 s period of background analysis, samples were spot ablated for 40 s at a 7 Hz repetition rate in an ultrahigh purity He–N₂ atmosphere using a 33/50μm beam and laser energy (at the sample surface) of 2.8 J/cm². Fe stoichiometry for pyrrhotite, pyrite, and magnetite, are 62.3%, 46.55%, and 72.36%, respectively. S stoichiometry for pyrrhotite and pyrite are 37.7% and 53.45%, respectively. ⁵⁷Fe was used as the internal reference isotope for GSD and BONN and for IMER (only for Te in magnetite). ³⁴S was used as the internal reference isotope for IMER for pyrite and pyrrhotite only for Te determination. S, Au and Ag were determined using BONN as the standard reference. All remaining elements determined against GSD-1g as the standard reference. No Fe concentrations are calculated by the data reduction scheme as it is a major element in most minerals and used as the primary reference isotope. The mass spectra were reduced using lolite 3.4 (Paton et al., 2011). bdl = below detection limit.

Table DR3 Chemical compositions and estimated P-T conditions of pyroxenes in the Liuhe xenoliths

Chemical compositions												
Sample	Lithology	Mineral	SiO ₂	TiO ₂	Al ₂ O ₃	FeO	MnO	MgO	CaO	Na ₂ O	K ₂ O	P ₂ O ₅
LH15-24	garnet amphibolite	Wo ₄₃ En ₄₁ Fs ₁₂	54.63	0.46	3.08	7.16	0.12	13.41	19.87	0.68	0.41	0.00
LH14-57	garnet amphibolite	Wo ₄₆ En ₃₇ Fs ₁₃	51.34	0.77	2.78	8.06	0.00	12.68	22.22	0.70	0.19	0.00
LH14-40	garnet amphibolite	Wo ₄₃ En ₃₂ Fs ₁₉	50.68	0.11	0.13	13.14	0.06	11.84	22.26	1.33	0.35	0.00
Ionic compositions												
Sample	Lithology	Mineral	Si	Al(iv)	Al(vi)	Ti	Cr	Fe ³⁺	Fe ²⁺	Mn	Mg	Ca
LH15-24	garnet amphibolite	Wo ₄₃ En ₄₁ Fs ₁₂	2.0025	0.0000	0.1331	0.0127	0.0000	0.0000	0.2222	0.0037	0.7328	0.7804
LH14-57	garnet amphibolite	Wo ₄₆ En ₃₇ Fs ₁₃	1.9363	0.0637	0.0599	0.0219	0.0000	0.0307	0.2229	0.0032	0.7129	0.8979
LH14-40	garnet amphibolite	Wo ₄₃ En ₃₂ Fs ₁₉	1.9516	0.0032	0.0000	0.0032	0.0000	0.2941	0.1187	0.0020	0.6797	0.9185
Sample	Lithology	Mineral	Na	K	Wo	En	Fs	Ac				
LH15-24	garnet amphibolite	Wo ₄₃ En ₄₁ Fs ₁₂	0.0483	0.0192	43.6600	41.0000	12.6400	2.7000				
LH14-57	garnet amphibolite	Wo ₄₆ En ₃₇ Fs ₁₃	0.0512	0.0091	46.8000	37.1500	13.3800	2.6700				
LH14-40	garnet amphibolite	Wo ₄₃ En ₃₂ Fs ₁₉	0.0993	0.0172	43.4800	32.1800	19.6400	4.7000				
Temperature results estimated with garnet-clinopyroxene Fe-Mg geothermometer / P-T results estimated with clinopyroxene geothermobarometer												
Sample	Lithology	P/MPa	T/°C		Sample	Lithology	T/°C	P/MPa	H/Km			
LH15-24	garnet amphibolite	1102.11	675.34		LH15-24	garnet amphibolite	1490.94	1354.12	44			
LH14-57	garnet amphibolite	1098.23	642.34		LH14-57	garnet amphibolite	1506.75	1560.34	46			

Note: Major element compositions of minerals were analyzed using a JXA-8230 electron microprobe at the Institute of Mineral Resources, Chinese Academy of Geological Sciences. The operating conditions were accelerating voltage of 15 kV for silicate and oxide. Natural minerals and synthetic oxides were used as standards. Matrix corrections were carried out using the ZAF correction program supplied by the manufacturer. Ionic composition were calculated using Bath (1952). The garnet-clinopyroxene Fe-Mg geothermometer from Ravna (2000) and the clinopyroxene geothermobarometer from Mercier (1980).

Table DR4 Chemical compositions of amphiboles in the xenoliths at Liuhe and Beiya

Chemical compositions												
Sample	Lithology	Mineral	SiO ₂	TiO ₂	Al ₂ O ₃	FeO	MnO	MgO	CaO	Na ₂ O	K ₂ O	P ₂ O ₅
BYB15-2-1	Amphibolite	edenite	44.59	0.30	13.55	14.14	0.45	10.04	11.12	2.89	0.50	0.00
LH15-24	Garnet amphibolite	pargasite	42.98	0.07	14.12	13.01	0.11	13.22	11.01	3.21	2.31	0.00
LH14-57	Garnet amphibolite	hastingsite	43.12	0.08	14.23	16.01	0.66	13.22	8.98	2.34	1.20	0.00
LH14-40	Garnet amphibolite	pargasite	43.35	1.68	14.97	15.75	0.05	9.87	10.45	2.58	0.27	0.00
Ionic compositions												
Sample	Lithology	Mineral	Si	Al ^{IV}	Al ^{VI}	Ti	Fe ³⁺	Fe ²⁺	Mn	Mg	Ca	Na
BYB15-2-1	Amphibolite	edenite	6.6430	1.3570	1.0230	0.0340	0.0000	2.2300	1.7130	0.0490	0.0560	1.7760
LH15-24	Garnet amphibolite	pargasite	6.2530	1.7470	0.6741	0.0077	0.0000	1.5829	0.0136	2.8672	1.7163	0.9055
LH14-57	Garnet amphibolite	hastingsite	6.2838	1.7162	0.7278	0.0088	0.0724	1.8788	0.0815	2.8720	1.4021	0.6612
LH14-40	Garnet amphibolite	pargasite	6.3308	1.6692	0.9075	0.1846	0.4133	1.5103	0.0062	2.1488	1.6352	0.7305
P result estimated with Al-in-amphibole barometer												
Sample	Lithology	P/MPa		H/Km								
BYB15-2-1	Amphibolite	832.00		27								
LH15-24	Garnet amphibolite	851.44		28								
LH14-57	Garnet amphibolite	862.34		28								
LH14-40	Garnet amphibolite	925.51		30								

Note: Major element compositions of minerals were analyzed using a JXA-8230 electron microprobe at the Institute of Mineral Resources, Chinese Academy of Geological Sciences. The operating conditions were accelerating voltage of 15 kV for silicate and oxide. Natural minerals and synthetic oxides were used as standards. Matrix corrections were carried out using the ZAF correction program supplied by the manufacturer. Ionic composition were calculated using Barth (1952).Al-in-amphibole barometer from Schmit (1992).

Table DR5 U-Pb ages of zircons from the xenoliths and their host rocks at Beiya and Liuhe

Spot No.	U ppm	Th ppm	Th/U	$^{207}\text{Pb}/^{206}\text{Pb}$		$^{207}\text{Pb}/^{235}\text{U}$		$^{206}\text{Pb}/^{238}\text{U}$		$^{206}\text{Pb}/^{238}\text{U}$	
				Ratio	1 σ	Ratio	1 σ	Ratio	1 σ	Age	1 σ
Liuhe garnet-amphibolite xenoliths											
1	297.58	164.63	0.57	0.06	1.40	1.12	2.10	0.13	1.60	760.00	11.00
2	1310.74	2393.70	1.89	0.05	3.80	0.04	4.20	0.01	1.60	35.04	0.56
3	221.39	13.66	0.06	0.05	8.80	0.01	99.00	0.01	2.70	36.90	1.00
4	857.58	86.36	0.10	0.07	0.82	1.15	1.70	0.13	1.50	774.00	11.00
5	232.94	126.27	0.56	0.06	1.60	1.21	2.20	0.13	1.60	813.00	12.00
6	1946.72	1298.75	0.69	0.05	3.00	0.04	4.30	0.01	1.50	37.41	0.57
7	1192.65	519.88	0.45	0.05	3.80	0.04	5.10	0.01	1.60	35.48	0.56
8	2548.46	1451.49	0.59	0.05	2.60	0.04	3.60	0.01	1.50	37.77	0.57
9	837.38	1169.89	1.44	0.05	4.70	0.03	7.40	0.01	1.70	34.88	0.58
10	515.78	424.21	0.85	0.05	6.50	0.01	89.00	0.01	2.50	35.53	0.90
11	821.98	513.01	0.64	0.07	0.85	1.21	1.80	0.13	1.50	806.00	11.00
12	227.09	87.02	0.40	0.07	1.70	1.20	3.10	0.13	2.10	807.00	16.00
13	2182.08	836.11	0.40	0.05	2.90	0.04	3.60	0.01	1.80	36.77	0.67
14	2146.77	766.05	0.37	0.05	2.90	0.04	3.70	0.01	1.50	36.07	0.55
15	844.56	907.70	1.11	0.04	4.80	0.03	5.10	0.01	1.70	35.75	0.60
16	192.08	21.19	0.11	0.06	9.00	0.04	27.00	0.01	5.30	35.50	1.90
17	1278.88	220.93	0.18	0.05	3.30	0.04	5.50	0.01	2.00	34.98	0.68
18	1583.23	648.65	0.42	0.05	4.90	0.04	9.80	0.01	2.00	36.68	0.73
Liuhe svenite (host)											
1	4078.18	1540.85	0.39	0.05	3.00	0.04	3.40	0.01	1.60	36.25	0.56
2	461.90	215.63	0.48	0.02	61.00	0.02	60.00	0.01	2.90	35.60	1.00
3	2038.90	1056.02	0.54	0.05	3.40	0.03	3.80	0.01	1.80	34.61	0.61
4	1642.81	1716.68	1.08	0.05	3.20	0.03	3.50	0.01	1.50	34.79	0.53
5	257.09	20.00	0.08	0.05	15.00	0.04	15.00	0.01	2.10	37.09	0.79
6	321.77	43.06	0.14	0.04	26.00	0.03	26.00	0.01	2.30	36.24	0.83
7	2878.02	5010.23	1.80	0.05	2.60	0.04	3.00	0.01	1.50	36.35	0.55
8	2846.01	3331.39	1.21	0.05	2.70	0.03	3.10	0.01	1.50	34.41	0.51

9	1069.23	678.24	0.66	0.03	54.00	0.02	54.00	0.01	2.70	33.65	0.93
Beiya amphibolite xenoliths											
1	34.18	4.60	0.14	0.07	3.30	1.07	5.30	0.12	2.90	723.00	20.00
2	51.93	15.27	0.30	0.08	2.60	1.14	4.80	0.12	2.70	743.00	19.00
3	297.50	255.37	0.89	0.07	1.10	1.22	2.60	0.13	2.30	796.00	17.00
4	139.02	53.71	0.40	0.07	3.60	1.23	4.40	0.13	2.40	816.00	19.00
5	55.62	9.80	0.18	0.06	8.60	0.99	9.00	0.12	2.70	738.00	19.00
6	173.58	39.68	0.24	0.07	2.80	1.18	3.70	0.13	2.40	783.00	17.00
7	145.69	87.26	0.62	0.06	3.50	1.09	4.30	0.13	2.40	764.00	17.00
8	188.57	226.92	1.24	0.07	3.10	1.18	4.00	0.13	2.50	778.00	18.00
9	9.00	2.04	0.23	0.08	34.00	1.37	34.00	0.12	5.40	747.00	38.00
Beiya monzogranite (host)											
1	508.86	187.39	0.38	0.04	56.00	0.03	56.00	0.01	3.50	39.90	1.40
2	591.72	211.97	0.37	0.04	5.90	0.03	6.50	0.01	2.70	36.48	0.96
3	583.27	185.74	0.33	0.05	5.80	0.04	6.30	0.01	2.60	38.18	0.98
4	1045.86	1347.50	1.33	0.05	16.00	0.04	16.00	0.01	2.60	38.70	1.00
5	322.30	108.87	0.35	0.04	15.00	0.03	15.00	0.01	3.10	37.40	1.20
6	337.35	106.96	0.33	0.05	6.90	0.04	7.40	0.01	2.80	37.70	1.00
7	1169.68	765.95	0.68	0.05	10.00	0.04	10.00	0.01	2.50	37.91	0.94

Note: Zircons from the volcanic rocks were dated on a SHRIMP II at the Beijing SHRIMP Center. Uncertainties in ages are quoted at the 95% confidence level (2σ). Spot diameter was 25mm for SHRIMP II. Common Pb corrections were made using measured ^{204}Pb . The calibration standard is Sri Lankan gem zircon standard (SL13), and the internal standard is the Australian National University zircon standard TEMORA 1.

Table DR6 Whole-rock chemical analyses of the xenoliths and host rocks of Beiya and Liuhe in the western Yangtze Craton

The xenoliths						
Location	Beiya	Beiya	Beiya	Liuhe	Liuhe	Liuhe
Sample	BYB15-2-1	BYB15-2-7	BYB15-2-9	LH151-17	LH151-11	LH151-8
Lithology	Amphibolite	Amphibolite	Amphibolite	Amphibolite	Amphibolite	Garnet amphibolite
wt%						
SiO ₂	50.2	49.9	50.6	49.0	49.2	45.8
TiO ₂	0.1	1.4	1.5	1.4	1.2	1.2
Al ₂ O ₃	14.3	14.2	14.4	17.3	17.1	11.8
Fe ₂ O ₃	4.7	4.6	3.7	4.4	6.1	3.9
FeO	7.6	7.7	7.7	6.5	3.6	6.8
MnO	0.2	0.2	0.2	0.2	0.2	0.1
MgO	5.2	5.3	5.2	7.3	8.6	12.4
CaO	1.4	1.4	1.4	3.9	3.7	10.0
Na ₂ O	1.4	1.3	1.3	3.7	4.3	2.3
K ₂ O	6.2	6.2	6.0	3.1	1.6	2.3
P ₂ O ₅	0.2	0.2	0.1	0.2	0.3	0.1
LOI	5.9	6.0	6.4	2.2	3.5	2.3
TFe ₂ O ₃	13.0	13.2	12.2	11.5	10.1	11.3
ppm						
Sc	40.6	40.4	39.3	27.3	24.7	47.3
Ti	855.9	8535.9	8697.9	8158.6	7288.0	7099.8
P	660.8	673.2	650.1	976.8	1505.6	322.2
V	232.7	237.4	223.5	196.2	160.8	366.4
Cr	320.4	318.8	312.7	92.8	17.5	352.6
Co	24.0	23.4	22.8	28.1	23.7	57.4

Ni	102.7	134.3	107.8	36.5	16.0	143.3
Cu	389.3	445.0	383.2	17.8	14.5	7.6
Au (ppb)	12	7	12	5	6	6
S	556.1	635.7	547.5	254.4	207.8	109.1
Zn	108.7	114.2	115.0	174.6	282.9	177.0
Ga	27.4	28.3	27.2	33.2	37.8	32.9
Rb	412.7	417.1	403.6	111.8	75.5	82.7
Sr	187.5	190.4	184.1	935.7	1415.7	590.8
Y	23.9	24.1	23.7	17.4	40.3	12.2
Zr	30.1	28.4	28.1	50.1	87.1	118.4
Nb	21.0	20.9	20.3	10.9	9.9	3.6
Ba	2489.3	2413.2	2403.3	802.1	500.1	1146.4
Hf	1.0	0.9	1.0	2.0	2.0	1.3
Ta	2.6	2.6	2.5	0.5	0.4	0.1
Pb	17.6	17.5	17.6	7.1	6.3	0.0
Th	2.9	2.8	2.8	2.2	0.9	10.4
U	3.9	3.9	3.8	0.7	0.4	0.8
La	32.3	32.8	31.5	19.0	44.4	9.8
Ce	71.1	71.0	69.2	40.0	91.7	20.6
Pr	8.3	8.4	8.1	4.9	12.1	2.7
Nd	27.9	28.1	27.4	18.1	45.1	11.5
Sm	6.7	6.7	6.5	4.2	10.9	3.0
Eu	2.0	2.0	2.0	1.6	2.5	0.9
Gd	5.2	5.3	5.2	3.5	8.5	2.8
Tb	0.8	0.8	0.8	0.5	1.3	0.4
Dy	4.4	4.4	4.4	3.1	7.0	2.5

Ho	0.9	0.9	0.9	0.7	1.5	0.5
Er	2.4	2.4	2.4	2.0	4.2	1.5
Tm	0.4	0.4	0.3	0.3	0.6	0.2
Yb	2.2	2.2	2.2	2.2	3.9	1.5
Lu	0.3	0.3	0.3	0.3	0.6	0.2
Location	Liuhe	Liuhe	Liuhe	Liuhe	Liuhe	Liuhe
Sample	LH151-13	LH14-8	LH14-9	LH14-10	LH14-11	LH14-53
Lithology	Garnet amphibolite					
wt%						
SiO ₂	42.0	44.2	44.1	44.1	44.0	43.8
TiO ₂	1.2	0.8	0.7	0.7	0.8	0.8
Al ₂ O ₃	11.7	11.3	11.3	11.3	11.3	12.4
Fe ₂ O ₃	6.8	4.3	4.3	4.5	4.4	6.4
FeO	6.1	8.3	8.2	8.2	8.2	5.2
MnO	0.2	0.2	0.2	0.2	0.2	0.3
MgO	14.7	14.6	14.8	14.8	14.7	15.2
CaO	8.3	8.9	8.8	8.9	8.9	6.6
Na ₂ O	1.5	2.3	2.4	2.4	2.3	2.3
K ₂ O	1.7	1.4	1.3	1.4	1.3	1.0
P ₂ O ₅	0.1	0.2	0.2	0.2	0.2	0.2
LOI	4.9	2.5	2.6	2.2	2.7	5.0
TFe ₂ O ₃	13.5	13.5	13.3	13.5	13.5	12.1
ppm						
Sc	41.9	221.8	222.5	216.5	222.6	175.0
Ti	6928.1	4588.7	4455.7	4445.1	4504.2	4887.9
P	479.5	1035.1	1005.3	1020.0	1007.6	938.6

	1	2	3	4	5	6
V	269.6	612.5	616.3	593.0	613.7	587.0
Cr	704.2	1284.9	1287.2	1238.3	1295.4	1944.7
Co	60.0	64.1	64.8	61.8	64.0	69.0
Ni	297.1	97.9	97.1	94.4	97.3	318.0
Cu	9.1	4.9	9.9	4.9	4.9	82.4
Au (ppb)	7	2	2	2	2.0	16
S	129.7	66.7	81.1	84.6	59.6	112.6
Zn	209.4	128.9	138.0	126.9	128.0	164.3
Ga	44.7	30.9	31.2	30.2	30.6	42.3
Rb	49.3	43.6	44.4	42.8	43.4	39.4
Sr	489.2	449.9	455.0	440.2	449.8	664.5
Y	18.0	15.8	15.8	15.1	15.6	24.2
Zr	73.6	39.6	39.2	36.5	37.4	24.0
Nb	2.3	2.2	2.2	2.1	2.4	3.9
Ba	400.7	243.2	242.7	235.7	243.8	325.1
Hf	2.2	3.7	3.7	3.6	3.7	9.0
Ta	0.1	1.3	1.3	1.2	1.2	0.8
Pb	6.6	1.2	1.1	1.0	1.0	1.4
Th	0.4	0.2	0.2	0.2	0.2	0.2
U	0.2	18.2	18.3	17.6	18.1	27.8
La	8.2	9.8	9.4	9.7	9.3	26.7
Ce	14.0	20.6	20.0	20.3	19.9	45.8
Pr	1.5	2.7	2.6	2.6	2.6	5.0
Nd	6.5	11.5	11.3	11.3	11.2	19.9
Sm	2.0	3.0	3.0	3.0	3.0	5.2
Eu	0.8	0.9	0.9	0.8	0.8	1.3

Gd	2.6	2.8	2.8	2.8	2.8	4.5
Tb	0.5	0.4	0.4	0.4	0.4	0.7
Dy	3.2	2.5	2.5	2.4	2.5	3.8
Ho	0.7	0.5	0.5	0.5	0.5	0.8
Er	2.2	1.5	1.5	1.4	1.5	2.1
Tm	0.4	0.2	0.2	0.2	0.2	0.3
Yb	2.6	1.5	1.5	1.4	1.5	2.0
Lu	0.4	0.2	0.2	0.2	0.2	0.3

Monzogranites at Beiya

Sc	4.4	4.7	4.8	3.8	4.5	5.8
Ti	1314.2	1433.8	1419.9	1342.6	1215.8	1671.1
P	511.9	617.6	533.7	566.7	490.1	623.9
V	29.8	32.2	38.5	28.6	36.1	47.9
Cr	3.2	0.1	7.8	0.5	12.0	18.5
Co	1.6	2.2	2.2	2.1	1.7	3.2
Ni	2.2	0.6	3.3	6.5	0.0	0.4
Cu	0.0	0.0	0.8	2.9	0.2	0.0
Au (ppb)	1	1	1	1	1	2
S	0.0	0.3	12.7	47.6	3.5	0.8
Zn	23.4	29.0	26.4	40.8	25.0	27.4
Ga	22.8	22.4	21.4	21.0	23.3	23.0
Rb	222.1	230.2	221.3	211.3	235.2	261.1
Sr	998.0	978.2	934.1	811.0	1008.1	990.8
Y	11.1	9.8	10.0	7.8	10.1	11.4
Zr	95.5	38.6	73.3	66.5	104.0	100.6
Nb	10.6	10.5	10.3	9.8	10.4	11.2
Ba	2157.0	2083.9	2058.7	1956.9	2084.5	2334.4
Hf	2.9	1.3	2.2	2.1	3.1	3.0
Ta	0.7	0.6	0.7	0.6	0.6	0.6
Pb	38.3	36.8	34.4	34.7	35.4	37.3
Th	11.2	11.9	10.6	10.0	12.6	11.4
U	2.5	2.3	2.3	2.1	2.8	2.6
La	21.3	21.2	19.1	17.8	20.7	20.2
Ce	37.7	37.8	35.6	32.2	37.3	39.6
Pr	3.9	3.9	3.9	3.1	3.8	4.2

Nd	14.5	14.3	13.7	10.3	12.0	14.0
Sm	3.4	3.4	3.1	2.1	2.6	3.0
Eu	1.2	1.2	1.1	1.0	1.2	1.3
Gd	2.4	2.4	2.3	1.8	2.3	2.6
Tb	0.3	0.3	0.3	0.3	0.3	0.4
Dy	1.8	1.7	1.7	1.3	1.7	1.9
Ho	0.3	0.3	0.3	0.3	0.3	0.4
Er	0.9	0.8	0.9	0.7	0.8	1.0
Tm	0.1	0.1	0.1	0.1	0.1	0.1
Yb	0.8	0.7	0.8	0.6	0.8	0.9
Lu	0.1	0.1	0.1	0.1	0.1	0.1

Syenites at Liuhe

Sample	LH14-58	LH14-1	LH14-8	LH14-9	LH14-10	LH14-53
Lithology	Syenite	Syenite	Syenite	Syenite	Syenite	Syenite
wt%						
SiO ₂	61.4	61.4	60.4	60.7	60.9	61.0
TiO ₂	0.7	0.7	0.7	0.7	0.7	0.8
Al ₂ O ₃	14.9	14.9	14.7	14.7	14.8	14.9
Fe ₂ O ₃	2.7	2.7	2.7	2.6	2.6	3.3
FeO	1.8	1.9	1.9	2.0	2.0	1.7
MnO	0.1	0.1	0.1	0.1	0.1	0.1
MgO	2.3	2.5	3.0	3.0	2.8	2.2
CaO	3.8	3.8	4.6	4.6	4.3	3.4
Na ₂ O	4.2	4.1	4.0	4.1	4.0	4.0
K ₂ O	6.3	6.2	6.0	6.0	6.0	6.5
P ₂ O ₅	0.4	0.4	0.4	0.4	0.4	0.4

LOI	1.0	1.0	1.1	0.7	1.1	1.2
TFe ₂ O ₃	4.7	4.7	4.8	4.8	4.7	5.1
ppm						
Sc	92.1	96.8	91.2	98.8	96.6	95.4
Ti	4226.5	4259.8	4417.8	4355.0	4340.5	4600.9
P	1895.0	1786.8	1827.2	1931.0	1823.6	1938.8
V	65.7	68.2	69.3	70.1	67.0	75.9
Cr	613.0	622.7	591.7	631.7	610.1	618.1
Co	14.0	14.0	13.7	14.3	13.9	18.0
Ni	34.4	34.4	32.6	34.4	33.2	39.2
Cu	4.3	7.2	4.0	7.5	7.1	44.4
Au (ppb)	2	1	1	2	1	1
S	61.2	34.8	40.2	40.8	56.4	43.7
Zn	45.0	45.5	44.6	46.7	45.4	48.9
Ga	17.6	17.8	16.7	18.2	17.6	18.1
Rb	188.7	176.9	158.7	182.5	174.5	215.0
Sr	570.4	565.8	503.5	575.8	546.1	593.0
Y	16.2	16.4	15.1	16.4	16.2	17.8
Zr	127.8	134.8	116.3	134.2	118.2	138.2
Nb	13.3	13.8	12.6	13.6	13.2	14.2
Ba	6.6	6.6	6.2	6.6	6.5	8.7
Hf	2053.6	2013.5	1902.9	2016.0	1969.7	2142.5
Ta	4.2	4.2	3.8	4.2	4.0	4.4
Pb	1.0	0.9	0.9	0.9	0.9	1.0
Th	28.3	29.8	28.2	30.4	29.3	24.3
U	8.7	8.3	7.6	8.3	8.2	8.5

La	27.8	27.3	24.8	28.2	26.8	32.6
Ce	57.4	56.8	53.3	57.5	56.4	61.5
Pr	6.7	6.6	6.1	6.6	6.5	7.7
Nd	26.0	25.0	23.3	24.8	24.7	28.1
Sm	5.9	5.9	5.5	5.8	5.8	6.6
Eu	1.7	1.7	1.6	1.7	1.7	1.9
Gd	4.7	4.7	4.4	4.7	4.7	5.3
Tb	0.6	0.6	0.6	0.6	0.6	0.7
Dy	3.4	3.4	3.1	3.4	3.4	3.7
Ho	0.7	0.7	0.6	0.7	0.7	0.7
Er	1.8	1.8	1.6	1.8	1.8	1.9
Tm	0.3	0.3	0.2	0.3	0.3	0.3
Yb	1.7	1.7	1.6	1.7	1.7	1.8
Lu	0.3	0.3	0.2	0.3	0.3	0.3

Note: Chemical compositions of whole rocks were measured at the Key Laboratory of orogenic belt and crustal evolution of the Ministry of education, Peking University. Major element compositions were analysed by X-ray fluorescence (BD-80) using fused glass disks. Trace element were determined by inductively coupled plasma-mass spectrometry (ICP-MS) using sample powders that were digested in a mixture of super-pure HNO₃ + HF in high-pressure Teflon bombs before being evaporated to near dryness and refluxed with super-pure HNO₃. Duplicate analysis of samples and rock standards (GSD9 and GSD12) yielded relative standard deviations that were <10% for most trace elements. Concentrations of copper obtained using the methods for the same samples generally agree to within 10% uncertainty (0.1ppm).

Gold was determined by inductively coupled plasma -mass spectrometry (ICP-MS). A prepared sample is fused with a mixture of lead oxide, sodium carbonate, borax and silica, inquarted with gold-free silver and then cupelled to yield a precious metal bead. The bead is digested at high power by microwave in dilute nitric acid. The solution is cooled and hydrochloric acid is added. The solution is digested at half power by microwave. The digested solution is then cooled, diluted with hydrochloric acid, homogenized and then analyzed for gold by inductively coupled plasma – mass spectrometry. The concentrations were determined by ICP-MS with an uncertainty of 1 ppb.

Table DR7 Zircon Lu–Hf isotope data of the Liuhe xenolith and syenite

Spot No.	$^{176}\text{Hf}/^{177}\text{Hf}$	$^{176}\text{Lu}/^{177}\text{Hf}$	$^{176}\text{Yb}/^{177}\text{Hf}$	Age (Ma)	$\epsilon\text{Hf(t)}$	$T_{\text{Dm}}(\text{Ga})$
The xenoliths						
1	0.2827	0.0004	0.0092	779.00	14.77	0.96
2	0.2824	0.0006	0.0092	774.00	4.47	1.16
3	0.2826	0.0018	0.0092	813.00	11.33	0.93
4	0.2824	0.0007	0.0092	982.00	9.34	1.15
5	0.2826	0.0012	0.0092	806.00	12.56	0.87
6	0.2823	0.0009	0.0092	760.00	0.66	1.30
7	0.2828	0.0007	0.0092	35.48	0.19	1.08
8	0.2828	0.0026	0.0091	34.88	3.36	0.79
9	0.2825	0.0011	0.0091	35.53	-7.1	1.38
10	0.2828	0.0014	0.0091	36.77	-0.01	1.43
11	0.2828	0.0007	0.0091	35.50	1.70	0.97
12	0.2829	0.0049	0.0090	35.04	4.90	0.89
13	0.2828	0.0007	0.0090	35.75	1.70	0.98
14	0.2828	0.0015	0.0090	36.03	3.01	1.43
15	0.2827	0.0012	0.0089	36.68	-2.96	1.14
16	0.2829	0.0000	0.0087	36.90	3.73	0.95
The host porphyries						
1	0.2828	0.0002	0.0245	36.25	2.15	1.01
2	0.2827	0.0010	0.0234	35.60	-1.67	0.91
3	0.2829	0.0005	0.0223	34.61	5.44	1.06
4	0.2827	0.0009	0.0211	34.79	-0.62	0.84
5	0.2828	0.0001	0.0197	37.09	3.01	0.79
6	0.2829	0.0005	0.0185	36.24	4.37	0.98
7	0.2828	0.0009	0.0173	36.35	0.47	0.87
8	0.2828	0.0005	0.0163	34.41	2.22	0.91
9	0.2827	0.0004	0.0151	33.65	-1.34	0.95

Note: Zircon Hf isotopic analysis was carried out in-situ on a Neptune multi-collector ICPMS equipped with a Geolas-193 laser-ablation system. (LA-MC-ICPMS) at the China University of Geosciences (Wuhan). Lu-Hf isotopic measurements were made on the same zircon grains previously analyzed for U-Pb isotope.

Table DR8 Chemical compositions of garnets in the Liuhe xenoliths

Chemical compositions												
Sample	Lithology	Mineral	SiO ₂	TiO ₂	Al ₂ O ₃	FeO	MnO	MgO	CaO	Na ₂ O	K ₂ O	P ₂ O ₅
LH151-1	Garnet amphibolite	Pyr ₂₃ Gro ₂₄ Alm ₅₀	35.56	0.07	23.01	25.11	0.1	6.54	9.67	0	0	0
LH14-57	Garnet amphibolite	Pyr ₂₄ Gro ₁₈ Alm ₅₁	36.63	0.08	21.68	26.14	0.66	6.63	8.66	0	0	0
LH14-40	Garnet amphibolite	Pyr ₂₆ Gro ₁₈ Alm ₄₁	36.82	0.84	19.11	23.64	0.4	6.83	11.6	0.06	0	0
Ionic compositions												
Sample	Lithology	Mineral	Si	Ti	Al	Cr	Fe ³⁺	Fe ²⁺	Mn	Mg	Ca	
LH151-1	Garnet amphibolite	Pyr ₂₃ Gro ₂₄ Alm ₅₀	2.7853	0.0041	2.1242	0	0.0162	1.6287	0.0066	0.7637	0.8116	
LH14-57	Garnet amphibolite	Pyr ₂₄ Gro ₁₈ Alm ₅₁	2.8554	0.0047	1.9918	0	0.1015	1.6026	0.0436	0.7705	0.7233	
LH14-40	Garnet amphibolite	Pyr ₂₆ Gro ₁₈ Alm ₄₁	2.8842	0.0495	1.7642	0	0.28	1.2687	0.0265	0.7976	0.9736	
Sample	Lithology	Mineral	Ura	And	Pyr	Spe	Gro	Alm	Other			
LH151-1	Garnet amphibolite	Pyr ₂₃ Gro ₂₄ Alm ₅₀	0	0.76	23.79	0.21	24.52	50.73	0			
LH14-57	Garnet amphibolite	Pyr ₂₄ Gro ₁₈ Alm ₅₁	0	4.85	24.54	1.39	18.19	51.04	0			
LH14-40	Garnet amphibolite	Pyr ₂₆ Gro ₁₈ Alm ₄₁	0	13.7	26.01	0.87	18.05	41.37	0			

Note: Major element compositions of minerals were analyzed using a JXA-8230 electron microprobe at the Institute of Mineral Resources, Chinese Academy of Geological Sciences. The operating conditions were accelerating voltage of 15 kV for silicate and oxide. Natural minerals and synthetic oxides were used as standards. Matrix corrections were carried out using the ZAF correction program supplied by the manufacturer. Ionic composition were calculated using Barth (1952)

Table DR9 Chemical compositions of micas in the Liuhe and Beiya xenoliths

Chemical compositions												
Sample	Lithology	Mineral	SiO ₂	TiO ₂	Al ₂ O ₃	FeO	MnO	MgO	CaO	Na ₂ O	K ₂ O	P ₂ O ₅
LH14-24	Garnet amphibolite	Biotite	34.99	1.47	16.47	16.83	0.37	17.15	0.03	0.37	5.32	0
LH14-57	Garnet amphibolite	Biotite	34.9	1.29	15.69	18.51	0.44	16.54	0.03	0.28	5.52	0
BYB15-2-1	Amphibolite	Biotite	38.39	0.9	15.53	14.61	0.32	15.15	0	0.26	9.18	0
Ionic compositions												
Sample	Lithology	Mineral	Si	Al ^{IV}	Al ^{VI}	Ti	Fe ³⁺	Fe ²⁺	Mn	Mg	Ca	Na
LH14-24	Garnet amphibolite	Biotite	2.6541	1.3459	0.1258	0.0839	0.1894	0.8781	0.0235	1.9388	0.002	0.0546
LH14-57	Garnet amphibolite	Biotite	2.6695	1.3305	0.0839	0.0745	0.1612	1.0227	0.0284	1.8861	0.0021	0.0408
BYB15-2-1	Amphibolite	Biotite	2.8773	1.1227	0.2487	0.0506	0.1559	0.7599	0.0204	1.6932	0	0.0373
Sample	Lithology	Mineral	K	MF	Fe ²⁺ +Mn	FM						
LH14-24	Garnet amphibolite	Biotite	0.5145	0.6399	0.9016	1.9045						
LH14-57	Garnet amphibolite	Biotite	0.5391	0.6087	1.0511	2.1472						
BYB15-2-1	Amphibolite	Biotite	0.8779	0.6439	0.7804	2.0226						

Note: Major element compositions of minerals were analyzed using a JXA-8230 electron microprobe at the Institute of Mineral Resources, Chinese Academy of Geological Sciences. The operating conditions were accelerating voltage of 15 kV for silicate and oxide. Natural minerals and synthetic oxides were used as standards. Matrix corrections were carried out using the ZAF correction program supplied by the manufacturer. Ionic composition were calculated using Barth (1952).

Table DR10 Chemical compositions of feldspars in the Liuhe and Beiya xenoliths

Chemical compositions								
Sample	Lithology	Mineral	SiO ₂	Al ₂ O ₃	CaO	Na ₂ O	K ₂ O	BaO
LH15-24	Garnet amphibolite	An _{0.73} Ab _{99.1} Or _{0.14}	67.11	21.99	0.13	9.95	0.02	0.00
LH14-57	Garnet amphibolite	An _{0.68} Ab _{99.9} Or _{0.38}	67.23	22.11	0.12	9.91	0.06	0.00
LH14-40	Garnet amphibolite	An _{1.31} Ab _{98.3} Or _{0.35}	72.61	21.52	0.17	7.08	0.04	0.00
BYB15-2-1	Amphibolite	An _{0.52} Ab _{8.2} Or _{91.24}	65.29	18.11	0.10	0.88	14.85	0.00
Ionic compositions								
Sample	Lithology	Mineral	Si	Al	Ca	Na	K	Ba
LH15-24	Garnet amphibolite	An _{0.73} Ab _{99.1} Or _{0.14}	2.9354	1.1335	0.0062	0.8440	0.0012	0.0000
LH14-57	Garnet amphibolite	An _{0.68} Ab _{99.9} Or _{0.38}	2.9339	1.1371	0.0058	0.8384	0.0032	0.0000
LH14-40	Garnet amphibolite	An _{1.31} Ab _{98.3} Or _{0.35}	3.0518	1.0661	0.0077	0.5770	0.0020	0.0000
BYB15-2-1	Amphibolite	An _{0.52} Ab _{8.2} Or _{91.24}	3.0187	0.9867	0.0050	0.0792	0.8761	0.0000
Sample	Lithology	Mineral	An	Ab	Or			
LH15-24	Garnet amphibolite	An _{0.73} Ab _{99.1} Or _{0.14}	0.7300	99.1200	0.1400			
LH14-57	Garnet amphibolite	An _{0.68} Ab _{99.9} Or _{0.38}	0.6800	98.9400	0.3800			
LH14-40	Garnet amphibolite	An _{1.31} Ab _{98.3} Or _{0.35}	1.3100	98.3400	0.3500			
BYB15-2-1	Amphibolite	An _{0.52} Ab _{8.2} Or _{91.24}	0.5200	8.2400	91.2400			

Note: Major element compositions of minerals were analyzed using a JXA-8230 electron microprobe at the Institute of Mineral Resources, Chinese Academy of Geological Sciences. The operating conditions were accelerating voltage of 15 kV for silicate and oxide. Natural minerals and synthetic oxides were used as standards. Matrix corrections were carried out using the ZAF correction program supplied by the manufacturer. Ionic composition were calculated using Barth (1952).

Table DR11 Zircon trace element compositions of Liuhe and Beiya xenoliths

Spot NO.	LH14-1	LH14-2	LH14-3	LH14-4	LH14-5	LH14-6
ppm						
Li	0.32	0.10	0.00	0.07	0.00	0.88
Be	0.06	0.00	0.00	0.00	0.00	0.00
B	0.04	1.58	1.52	0.00	0.00	0.96
Na ₂ O	0.00	22.12	2.40	0.00	0.00	0.00
MgO	0.00	55.34	157.06	0.00	0.00	2.36
Al ₂ O ₃	0.00	196.12	235.93	0.00	0.00	5.04
SiO ₂	329595.04	334286.72	338594.87	331492.29	340139.06	334825.91
P ₂ O ₅	875.37	644.71	980.46	795.69	335.14	558.81
K ₂ O	0.00	50.82	22.07	0.00	0.00	0.00
CaO	79.08	147.65	111.87	52.38	183.36	150.51
Sc ₂ O ₃	1303.70	1274.04	1210.80	1430.95	1363.88	1225.18
TiO ₂	21.01	24.52	18.89	12.65	1.66	22.43
V	0.93	0.24	0.76	0.16	0.14	0.28
Cr	6.18	1.02	1.22	0.00	4.71	0.35
MnO	0.00	2.90	3.88	0.85	0.00	0.82
TFe ₂ O ₃	0.00	159.84	284.24	0.00	5.08	20.42
Co	0.00	0.04	0.02	0.00	0.00	0.03
Ni	0.00	0.04	18.11	4.61	7.89	19.66
Cu	0.56	0.41	0.40	0.15	0.58	1.06
Zn	0.82	1.85	0.09	0.82	0.45	0.27
Ga	0.35	0.00	0.09	0.15	0.13	0.55
Ge	0.00	1.82	0.00	0.00	2.80	5.14
As	0.59	0.00	0.33	0.00	0.00	0.63
Rb	0.72	0.33	0.72	0.80	0.09	2.06
Sr	1.47	1.74	1.61	1.35	1.05	2.35
Y	1481.70	508.47	1104.36	1568.90	183.63	6215.42
ZrO ₂	652794.72	650762.18	644789.57	654268.50	645572.47	637660.80
Nb	4.42	4.03	6.74	4.50	3.83	16.38
Mo	0.34	0.28	0.47	0.39	0.55	0.44
Ag	39.71	39.51	40.51	40.98	44.04	44.29
Cd	7.32	8.21	9.29	7.99	8.40	7.60
In	0.04	0.00	0.00	0.04	0.01	0.02
Sn	86.40	34.88	24.38	27.06	28.91	541.45
Sb	0.03	0.13	0.00	0.00	0.00	0.00
Cs	0.00	0.00	0.02	0.04	0.08	0.02
Ba	0.02	2.48	0.88	0.00	0.18	0.00
La	0.02	0.20	0.16	0.04	0.03	0.33
Ce	4.40	5.14	11.82	8.06	0.51	517.70
Pr	0.19	0.13	0.08	0.20	0.00	0.92
Nd	3.53	1.02	1.16	3.59	0.05	10.00
Sm	7.12	2.20	2.71	7.99	0.31	17.03

Eu	0.23	0.69	0.45	2.73	0.25	11.22
Gd	40.91	11.63	22.17	42.89	3.28	111.73
Tb	12.00	3.82	7.73	13.03	1.15	36.69
Dy	136.42	44.80	98.70	151.37	15.40	441.21
Ho	54.20	18.02	42.06	60.72	6.69	181.09
Er	195.16	66.75	159.02	220.02	23.01	686.76
Tm	41.94	14.65	36.13	47.81	5.11	156.15
Yb	376.07	138.98	348.75	444.63	47.59	1520.41
Lu	69.48	29.98	63.88	79.45	13.98	229.25
HfO ₂	11912.51	11155.57	11373.62	8922.69	11812.71	7975.51
Ta	1.16	0.67	1.54	0.71	0.35	0.57
W	0.34	0.57	0.19	0.16	0.18	0.37
Au	0.15	0.29	0.15	0.08	0.07	0.18
Pb	4.96	2.75	4.17	5.93	0.32	5.60
Th	327.07	65.86	54.40	107.31	6.37	3550.46
U	511.17	202.15	147.49	169.25	174.55	3214.69
Th/U	0.64	0.33	0.37	0.63	0.04	1.10
Spot NO.	LH14-7	BYB15-1	BYB15-2	BYB15-3	BYB15-4	BYB15-5
ppm						
Li	0.00	7.10	7.45	60.00	0.82	0.14
Be	0.00	0.00	0.00	1.27	0.00	0.62
B	0.00	0.00	1.24	1.64	0.00	2.09
Na ₂ O	80.37	0.00	29.16	0.00	393.82	0.00
MgO	0.00	0.00	0.00	0.78	523.77	46.63
Al ₂ O ₃	569.63	550.59	341.58	237.39	1350.64	412.51
SiO ₂	350994.32	327925.71	324088.73	300035.74	314956.01	320870.20
P ₂ O ₅	825.80	693.71	1203.19	3343.99	430.44	500.02
K ₂ O	240.37	0.00	101.11	0.00	88.02	11.72
CaO	178.80	129.57	148.46	30.91	770.20	201.82
Sc ₂ O ₃	2304.10	1222.08	1276.34	1431.51	1336.05	1327.80
TiO ₂	220.13	77.94	8.19	9.97	45.84	17.79
V	0.64	0.36	0.24	0.33	1.75	0.25
Cr	4.26	0.00	3.54	4.53	7.97	0.00
MnO	1.90	1.62	3.02	1.00	15.29	1.15
TFe ₂ O ₃	93.57	95.34	107.35	18.77	966.47	572.85
Co	0.10	0.01	0.02	0.00	0.35	0.02
Ni	4.18	14.41	1.24	0.00	0.00	0.00
Cu	0.59	0.36	0.25	3.93	1.44	0.52
Zn	0.82	1.22	1.30	4.49	2.11	0.70
Ga	0.77	0.34	0.13	0.31	0.40	0.00
Ge	3.60	0.07	0.00	0.00	0.00	0.00
As	0.41	0.56	1.06	0.25	0.00	6.17
Rb	2.36	0.86	1.55	2.83	0.57	0.92
Sr	1.67	1.65	1.94	2.88	2.57	2.15

Y	2028.69	1706.51	2690.58	5215.51	380.31	1855.08
ZrO ₂	621339.34	656076.52	656899.88	667855.83	665168.99	659084.45
Nb	70.71	3.89	10.26	7.57	5.50	9.94
Mo	0.51	0.04	0.35	0.48	0.55	0.24
Ag	43.54	34.23	36.27	31.36	34.65	34.00
Cd	8.33	7.09	7.41	6.94	5.22	6.48
In	0.20	0.07	0.04	0.01	0.00	0.05
Sn	430.10	42.93	88.15	318.30	20.54	124.30
Sb	0.08	0.00	0.08	0.06	0.00	16.39
Cs	0.16	0.05	0.01	0.00	0.00	1.26
Ba	1.02	0.00	4.99	0.42	0.60	1.03
La	1.09	0.11	0.12	0.16	0.11	0.32
Ce	265.33	9.40	17.86	14.48	4.32	64.50
Pr	6.41	0.38	0.25	0.20	0.09	0.77
Nd	63.92	5.54	4.70	2.57	0.51	12.43
Sm	67.13	8.03	10.18	8.72	0.93	22.50
Eu	35.22	2.01	1.97	0.94	0.15	11.95
Gd	176.57	40.72	62.99	75.75	5.89	94.41
Tb	38.81	12.84	20.56	32.49	1.91	24.12
Dy	306.56	154.47	250.73	440.66	24.65	223.38
Ho	81.51	63.19	101.99	193.72	13.10	72.51
Er	215.48	235.13	367.80	766.83	67.28	220.90
Tm	40.51	54.53	80.25	179.66	23.11	45.69
Yb	348.70	537.94	762.60	1731.26	316.04	392.25
Lu	49.59	101.56	127.28	328.10	78.25	67.67
HfO ₂	9039.99	9665.72	9948.73	15228.85	12760.34	11019.06
Ta	3.81	0.49	4.19	3.71	0.72	0.74
W	0.12	0.12	0.25	0.74	0.33	0.72
Au	0.09	0.93	0.87	1.11	8.76	1.59
Pb	6.31	3.22	7.49	21.34	11.65	2.04
Th	7153.22	246.75	599.58	330.14	36.48	1795.55
U	2648.54	262.06	564.50	2009.54	134.49	817.58
Th/U	2.70	0.94	1.06	0.16	0.27	2.20

Note: Zircon trace element were analyzed using ICP-MS at National Research Center for Geoanalysis, Chinese Academy of Geological Sciences. The samples were decomposed in mixed acid (HF-HNO₃-HClO₄) in sealed Teflon bombs. After complete digestion, dilution with 3% m/m HNO₃ was carried out with a dilution rate of 200 m/m. A proportion of this solution (5 ml) was transferred to other cells and 5 ml of a solution containing Lu as an internal standard was added. After mixing, solutions were analyzed the instrument, using the following working conditions: radio frequency (RF) power = 1000 W, carrier gas flow = 1.25 l min⁻¹, cool gas flow = 15.0 l min⁻¹, auxiliary gas flow = 1.50 l min⁻¹, integration time = 5 s, repeated data collection = 8.